

Optical Spectroscopy of Diffuse Ionized Gas in M31

B. Greenawalt and R.A.M. Walterbos¹

Astronomy Department, Box 30001, Department 4500, New Mexico State University, Las Cruces,
NM 88003

and

R. Braun¹

Netherlands Foundation for Research in Astronomy, Radiosterrenwacht, P.O. Box 2, 7990 AA
Dwingeloo, The Netherlands

ABSTRACT

We have obtained sensitive long-slit spectra of Diffuse Ionized Gas (DIG) in the Andromeda Galaxy, M31, covering the wavelength range of 3550-6850Å. By co-adding extracted DIG spectra, we reached a 1σ uncertainty of 9.3×10^{-19} ergs s⁻¹ cm⁻² arcsec⁻² corresponding to .46 pc cm⁻⁶ in Emission Measure. We present average spectra of DIG at four brightness levels with Emission Measures ranging from 9 to 59 pc cm⁻⁶. We present the first measurements of [OII]λ3727 and [OIII]λ5007 of the truly diffuse ionized medium in the disk of an external spiral galaxy. We find that $I_{[\text{OII}]} / I_{\text{H}\alpha} = .9 - 1.4$. The [OIII] line is weak ($I_{[\text{OIII}]} / I_{\text{H}\beta} = .5$), but it is stronger than found for the Galactic DIG. Measurements of [NII]λ6583 and [SII](λ6717 + λ6731) are also presented. The [SII] lines are clearly stronger than typical HII regions ($I_{[\text{SII}]} / I_{\text{H}\alpha} = .5$ compared to .2), confirming various imaging studies of spiral galaxies. Overall, the line ratios are in agreement with predictions of photoionization models for diffuse gas exposed to a dilute stellar radiation field, but the line ratios of the DIG in M31 are somewhat different than observed for Galactic DIG. The differences indicate a less diluted radiation field in the DIG of M31's spiral arms compared to DIG in the Solar Neighborhood of the Milky Way. Turbulent mixing layers can contribute at most 20% of the ionization budget of the DIG, with lower percentages producing better fits to the observed line ratios. We have also detected HeI λ5876 emission from the brightest DIG in M31. The HeI line appears to be stronger than in the Galactic DIG, possibly indicating that most of the Helium in the bright DIG in M31 is fully ionized. However, this result is somewhat tentative since bright night sky lines hamper an accurate measurement of the HeI line strength.

¹Visiting Astronomer, Kitt Peak National Observatory, National Optical Astronomy Observatories, which is operated by the Association of Universities for Research in Astronomy (AURA) under cooperative agreement with the National Science Foundation.

Subject headings: galaxies: individual (M31) — galaxies: ISM — galaxies: spiral — ISM: structure

1. Introduction

For years, it has been known that extensive quantities of ionized hydrogen, not restricted to the immediate vicinity of high mass stars, exists in the Milky Way and several external galaxies. In the Galaxy, this gas is referred to as the Reynolds Layer (Reynolds 1991), while a more general description is Diffuse Ionized Gas (DIG) or the Warm Ionized Medium (WIM). DIG is seen as a thick layer above the disk of some edge on galaxies (eg. NGC 891: Rand 1996, Rand et al. 1990, Dettmar 1990, Dettmar & Schulz 1992, Keppel et al. 1991; NGC 4631: Dettmar 1992, Rand et al. 1992, Golla et al. 1996; and NGC 55: Ferguson et al. 1996a), as bright filaments in some irregular galaxies (Hunter & Gallagher 1996, 1992, & 1990, Hunter 1996, 1994a, Hunter et al. 1993), and as both diffuse and filamentary regions in several nearby “face-on” spiral galaxies (M31: Walterbos & Braun 1994, Hunter 1994b; M33: Hester & Kulkarni 1990, Greenawalt & Walterbos 1997a, Hunter 1994b; M51 & M81: Greenawalt & Walterbos 1997b; Sculptor Group galaxies: Hoopes et al. 1996, Ferguson et al. 1996b). In all cases, most of the DIG is found to be concentrated in regions of star formation, although isolated patches and filaments are found as well.

While observations of this component of the ISM have occurred with increasing frequency over the last 5 years, the ionization and overall 3-D morphology are still poorly understood. Various models have been suggested to account for the ionization: Lyman continuum photons emitted by OB stars (Mathis 1986, Domgörgen & Mathis 1994, Dove & Shull 1994, Miller & Cox 1993), turbulent mixing of hot and cool gases (Slavin et al. 1993), shocks from supernovae (see Reynolds 1984), and decaying dark matter (Sciama 1990, 1993, & 1995). Each of these models has its difficulties, with some problems being more severe than others. Photoionization models need large mean free paths for ionizing radiation, requiring the ISM to be perhaps more porous than previously thought. However, these models are most attractive from an energetics standpoint, although still requiring up to 40% of the ionizing radiation from OB stars. Conversely, shocks from supernovae and mixing layer models are unable to ionize all of the DIG, even if all the energy of supernovae were available. Also, emission line ratios of the emitting gas constrain the shock speeds to an uncomfortably narrow range ($\sim 80 \pm 10$ km/s) (Raymond 1979, Shull & McKee 1979). Decaying dark matter models require other sources of ionizing radiation to produce [NII]($\lambda 6548 + \lambda 6583$), HeI($\lambda 5755$), and [OIII]($\lambda 4959 + \lambda 5007$) (Sciama 1995), and should be considered speculative.

Observations of DIG in external galaxies have largely been accomplished with imaging of H α and [SII]($\lambda 6717 + \lambda 6731$), and recently, [OII] $\lambda 3727$, the blend of [OII]($\lambda 3726 + \lambda 3729$), through narrow band (25-75Å) filters (eg. Walterbos & Braun 1992, 1994; Ferguson et al. 1996a,b; Rand et al. 1990, 1992). Spectroscopic studies have been mostly confined to thick ionized layers above edge-on systems (Rand 1996, Golla et al. 1996) and filaments in irregulars (e.g. Hunter and

Gallagher 1996). The imaging studies have shown that a surprisingly consistent fraction (30-50%) of the total $H\alpha$ emission from spirals arises in the DIG. Some recent studies have suggested that the $[SII]/H\alpha$ intensity ratio increases with decreasing surface brightness. To better test ionization models, observations of other lines are important. While the observations of edge-on systems address the ionization and excitation state of the gas *above* galactic disks, they do not provide information on the line ratios *in* the galactic disks.

Here we present the initial results from a spectroscopic study of the emission from faint DIG in the non-edge-on spiral M31. The spatial resolution provided by M31’s proximity allows clear separation of DIG regions from HII regions. This lack of “confusion” aids in the observation of faint DIG. Previous sensitive $H\alpha$ imaging (Walterbos & Braun 1992, 1994) over most of the NE half of the galaxy provided valuable complimentary information and aided the acquisition and interpretation of these spectroscopic data.

In §2 we review the observational procedures and data reduction techniques. The observed forbidden line ratios are presented in §3, along with the detection of HeI and temperature estimates. In §4 we compare the predictions of ionization models to our observations. In §5 we discuss the observed characteristics of DIG in M31 to that in other galaxies. Finally, §6 contains a summary of our results.

2. Observations and Data Reduction

The spectra were obtained using the RC spectrograph on the Mayall 4-m telescope at Kitt Peak National Observatory on Nov. 3-5, 1991. The detector was a Tek CCD chip with 1024x1024 pixels, each 0.69 arcseconds (2.3 pc for M31) on a side. A slit of about 6 arcminutes length and 2 arcseconds width was used. The slit was rotated to provide the best compromise between the ideal parallactic angle and the desire to include many interesting objects on the slit, eg. HII regions, SNRs, and regions of diffuse ionized gas. These objects were identified on $H\alpha$ and $[SII]$ images obtained by Walterbos and Braun (1992). Sixteen different slit positions were observed in the NE half of M31. They are mainly concentrated in the spiral arms, over a range in galactic radii of 5 to 15 kpc, with a concentration of slit locations in the 10 kpc star formation “annulus”. The locations of the slits on the sky will be presented elsewhere, when we discuss the results for the individual spectra (Greenawalt et al. 1997); here we are concerned only with the average DIG spectra at various brightness levels. We used the KPC-10A grating, with 316 lines/mm which is blazed to provided maximum sensitivity at 4000\AA in first order. The final dispersion with this grating was $2.77\text{\AA}/\text{pixel}$. For each slit position the grating was toggled between two tilt angles, centering the spectra on 4950\AA and 5500\AA , to provide a blue and a red spectrum. This strategy provided wavelength coverage from 3550\AA - 6850\AA with considerable overlap. At each tilt angle, two 15 minute object spectra and one wavelength calibration spectrum were taken.

Standard IRAF tasks were used to reduce the data. The CCD DC offset was removed by

fitting the overscan regions on each spectrum. Any residual bias structure was removed using a combination of bias images taken each night. Pixel-to-pixel variations were corrected using spectra of a quartz lamp illuminating the dome. Cosmic rays were edited out manually to insure that no spectral features were altered.

Each pair of spectra for a particular slit position and central wavelength were averaged together. The wavelength solution for the matching spectrum of a HeNeAr arc lamp was determined, then applied to the object spectrum. The spectra were flux calibrated using a standard star spectrum obtained during the night. One standard star observation from each night was used to calibrate the entire nights data. The sky conditions were clear, but we did not rigorously verify if conditions were photometric. Nevertheless, the emission measures we derive on the average spectra (see below) agree well with those derived from the corresponding image sections on the $H\alpha$ images obtained by Walterbos & Braun (1994).

The detector focus was slightly poorer at the edge of the field compared to the center of the field. A spectral line was therefore broader and the peak brightness was lower at the edge of the field. Because of this structure in the night sky lines, fitting a constant or a linear fit to a night sky line resulted in unacceptably large residuals when attempting a standard sky subtraction. Tests showed that a 7th order polynomial fit provided the best subtraction of the 4 brightest night sky lines, $[OI]\lambda 5577$, $NaI(\text{blend})\lambda\lambda 5890 + 5896$, $[OI]\lambda 6300$, and $[OI]\lambda 6364$. Since these lines have no underlying M31 nebular emission, such a high order fit was well constrained. Removal of the other night sky lines is more complicated, however.

The strengths of individual night sky lines vary in differing amounts from one spectrum to the next. Thus even if we had observed separate blank-sky spectra, we would not have obtained good removal of all night sky lines in individual M31 spectra. The standard technique, of fitting on background regions in each individual spectrum could only be used in a limited way, since the emission from DIG in M31 extended over most of the slit, severely limiting the choice of “background” regions. In addition, with only a few background regions per spectrum a high order fit to the sky features was not possible. Therefore, we were forced to develop an alternative background subtraction method. This method took advantage of the fact that the structure of a night sky line did not vary as the strength of the line changed.

In what follows it may be useful to remember that the dispersion direction is sometimes referred to as “columns” or “vertical direction”, while the spatial direction along the slit is referred to as “rows”. All spectra were shifted to a common wavelength grid. First, the four brightest night sky lines were removed from the individual spectra, using the following method. The smoothly varying continuum in each spectrum was removed by subtracting a median filtered version of the original spectrum. Continuum sources, such as foreground stars & M31 emission, were removed as well in this step, leaving only the individual fainter night sky lines and the nebular emission features in the spectra. The smoothly varying continuum of the sky brightness was determined by applying a rectangular median filter box of 1×151 pixels, with the long dimension aligned

with the dispersion axis. On the spectrum with the continuum subtracted, a 7th order 1-D polynomial was fit to each of the rows containing emission from the four bright sky lines. These fits were then removed from the original spectrum. The method was iterated until the sky line subtraction produced no noticeable depressions in the continuum level at the wavelength of the lines. Removing the brightest lines first was required to avoid the creation of large dips near the locations of these lines when subtracting the median filtered image. All subsequent steps were performed on the spectra from which the four bright night sky lines had been removed.

Next, we determined templates of the remaining night sky lines, which could then be used to remove these lines from the spectra. For this purpose, we selected the two spectra with the least amount of nebular emission from M31, hence with the most “background” regions on which the night sky lines could be fit. We again first removed the smoothly varying continuum, as described above. On each spectrum, we then selected background regions, to which 3rd order 1-D polynomials were fit, row by row. Higher order fits were not possible given the extent along the slit of the background regions available. The polynomial fits to each spectrum were written out as a template spectrum of night sky lines. The resulting two templates were averaged together to produce a final night sky line template.

The final step consisted of removing the night sky lines from all spectra using this template. To do this, we again determined the smoothly varying continuum for each spectrum using the median filter as described above, and subtracted this from the original spectrum. We then identified background regions on all spectra. For each row, we determined the mean intensity in the background regions, and the corresponding mean intensity in the night sky template for the same regions. This provided the scaling factor required to create an individual night sky template for each spectrum; this was then subtracted from the original spectrum, with the continuum still in it, to produce the final M31 spectra. Even in cases where the emission filled most of the slit, good sky subtraction was obtained this way. By subtracting the templates from the original spectra, no potential artifacts introduced by the median filtering can affect the data. With the night sky lines removed, only a smoothly varying background component, due to continuum emission from M31 and the night sky, was left to remove. A linear fit to the background regions along each row proved sufficient to remove this final background component.

3. Results

3.1. Representative DIG spectra

After the background was subtracted, we identified the various emission-line objects covered by each slit location, using the narrow-band images of the fields (Walterbos and Braun 1992). Based on morphology and brightness level, we classified 54 apertures as containing DIG. These ranged from roughly 10 to 60 pixels in extent, with a mean value of 23.5 pixels (54 pcs). Apertures containing HII regions, Supernova Remnants, candidate Luminous Blue Variables, Wolf-Rayet

stars and other objects were also extracted. These will be discussed elsewhere (Walterbos et al. 1996, Galarza et al. 1997).

All extracted spectra were shifted so the emission lines were at their respective rest wavelengths. This step removed the systemic velocity of M31 and any rotational velocity differences between the DIG locations. Using gaussian fits to line profiles in the task SPLOT, the $H\alpha$ flux was measured for each DIG aperture and then converted to average intensity using the number of summed pixels in each aperture. The Emission Measures (EM) derived from the $H\alpha$ surface brightness, assuming $T_e = 10^4\text{K}$, of the DIG within the 54 apertures ranged from $12\text{-}71 \text{ pc cm}^{-6}$. After ordering the apertures by decreasing surface brightness, they were separated into 3 groups of 18 apertures each. The 1D spectra within each group were then combined to produce representative spectra of “Bright”, “Moderate”, and “Faint” DIG, with EMs of 58.4, 33.8, and 17.7 pc cm^{-6} , respectively. In addition, twelve DIG regions located well away from any bright HII regions or filaments were combined to produce a representative spectrum of DIG “Far” from HII regions. This DIG had an average $\text{EM} = 22.6 \text{ pc cm}^{-6}$. To compliment these spectra, we extracted 26 apertures of regions with very faint emission which showed only marginal detection of $H\alpha$ in individual cases. These were shifted using adjacent apertures of brighter emission as reference, then combined to produce a representative spectrum of the “Very Faint” DIG with emission measure of 9.1 pc cm^{-6} . The 1σ noise in all final co-added spectra was roughly $9.3 \times 10^{-19} \text{ ergs s}^{-1} \text{ cm}^{-2} \text{ arcsec}^{-2}$, corresponding to an EM of $.46 \text{ pc cm}^{-6}$. This noise level is low compared to the faintest DIG we extracted from the spectra, mainly because the noise in individual spectra is much higher, so identifying regions at these faint levels is not trivial. In addition, since emission may fill most of the slits completely, extracting fainter spectra introduces a systematic uncertainty in the derived line ratios due to possible subtraction of a low-level (estimated by Walterbos & Braun (1994) to be no higher than $\text{EM} = 3 \text{ pc cm}^{-6}$) genuine DIG component. The low noise in the co-added spectra implies that we have excellent S/N even for the “Very Faint” DIG.

Table 1 contains the line ratios for each of these combined spectra. The quoted “uncertainties” in the surface brightness of the combined spectra correspond to the 1σ rms spread in the distribution of surface brightnesses of the individual spectra. In the case of the “Very Faint” DIG, this number is an estimate, since surface brightnesses for individual spectra were not measured. Uncertainties quoted for line ratios reflect 1σ errors determined from the combined spectra. We will report on results for the individual spectra in a different paper (Greenawalt et al. 1997). It is important to point out that the intrinsic spread in the line ratios from one region to another is much larger than the quoted uncertainties here, which are derived from the co-added spectra. Thus there is significant variation in line ratios across the DIG but globally the line ratios vary little.

The measured emission line intensities from each combined spectrum were corrected for reddening using the Balmer decrement and a standard Galactic extinction curve (Savage & Mathis 1979). The ratio $I_{H\alpha}/I_{H\beta}$ was 4.4 for the “Very Faint” DIG spectrum and roughly 3.6 for others, compared to an unreddened value of 2.86 for 10^4 K gas. Because the absorbing material may well

be mixed with the DIG, we calculated corrected line ratios for both a foreground screen model and a model consisting of a Galactic foreground dust screen and a homogeneous mixture of dust and DIG in M31. For a foreground dust screen, the extinction implied by the observed line ratios is $A_V \simeq .7$ ($A_V \simeq 1.2$ for the “Very Faint” DIG), roughly twice the foreground Galactic extinction, for which $E(B-V) = .1$ (e.g., Walterbos & Schwing 1987). The model, with a component of dust and DIG mixed in M31, suggests the dust column from this component alone would correspond to an $A_V \simeq .6-1.1$ if it were a foreground screen ($A_V = 3.1$ for the “Very Faint” spectrum), in addition to the foreground Galactic extinction, $A_V = .3$. Because of the dust distribution in this model, the corrected line ratios are actually slightly smaller compared to a model of only foreground extinction, in spite of the increased estimation of the total extinction. In the most extreme case of $I_{[\text{OIII}]} / I_{\text{H}\alpha}$, the line ratios are reduced by less than 5% (less than 10% for the “Very Faint”), roughly consistent with our 1σ error estimation. Because the exact distribution of dust has little effect on the corrected line ratio in this case, we quote corrected line ratios assuming the extinction arises within a foreground dust layer. The reddening corrected ratios of other Balmer line ratios, in particular, $\frac{\text{H}\gamma}{\text{H}\beta}$ and $\frac{\text{H}\delta}{\text{H}\beta}$ for all DIG spectra are consistent with the expected values for unreddened 10^4 K ionized gas.

3.2. Forbidden line ratios

Portions of the observed spectra around $\text{H}\alpha$ are shown in Fig. 1. The figure gives a good indication of our signal-to-noise and wavelength resolution. Night sky lines just blueward of $\text{H}\alpha$ caused some problems with the accurate determination of both the strength of the $[\text{NII}]\lambda 6548$ line and the baseline level; all $[\text{NII}]$ measurements therefore refer to the $\lambda 6584$ line. We find a constant $I_{[\text{NII}]\lambda 6583} / I_{\text{H}\alpha}$ ratio of .35 for all four brightness levels of DIG, but a slightly higher value of .40 for DIG “Far” from HII regions. This is similar to that measured for HII regions and for the Reynolds layer in our Galaxy (Reynolds 1990).

The strength of the $[\text{SII}]\lambda 6717 + \lambda 6731$ lines relative to the $\text{H}\alpha$ line has been recognized for some years to be different in DIG versus HII regions. Many imaging programs have used the value of $I_{[\text{SII}]} / I_{\text{H}\alpha}$ along with the brightness of $\text{H}\alpha$ to distinguish DIG in nearby galaxies (e.g. Walterbos and Braun 1994, Hoopes et al. 1996, Ferguson et al. 1996b). Our spectra show values of $I_{[\text{SII}]} / I_{\text{H}\alpha}$ in the range of .40-.50, which is significantly larger than the average value of .25 observed in HII regions (Walterbos and Braun 1994, also Fig. 4). The ratio obtained for the “Far” DIG is .60, considerably higher. There appears to be a trend of increasing ratio with decreasing surface brightness, both in the combined spectra and in the individual spectra before combination (Greenawalt et al. 1997).

Figure 2 shows a large portion of the blue spectra. Wavelengths shortward of 4200\AA were observed only in the blue spectra, and therefore have lower signal-to-noise. The decline of detector sensitivity and reduced atmospheric transmission in this wavelength region also have a negative effect on the signal-to-noise. In spite of these facts, we clearly detect the $[\text{OII}]$ doublet at $\lambda 3727$ in

all DIG spectra. The reddening corrected $I_{[\text{OII}]} / I_{\text{H}\beta}$ ratio is 2.6 for the “Bright” and “Moderate” spectra, 3.4 for the “Faint” spectrum, and 4.1 for the “Very Faint” spectrum. This translates to $I_{[\text{OII}]} / I_{\text{H}\alpha} = .9, 1.2, \text{ and } 1.4$, respectively. The ratio obtained for the “Far” DIG is basically the same as for the “Faint” DIG. The $[\text{OIII}]\lambda 4959$ line is weak and not seen in the spectra of the faintest DIG, but the stronger of the doublet, $[\text{OIII}]\lambda 5007$, is accurately measured in all spectra. The $I_{[\text{OIII}]\lambda 5007} / I_{\text{H}\beta}$ ratio for DIG in M31 ranges from .35 to .60. Note that the $[\text{OI}]\lambda 6300$ line, if present, could not have been detected in M31 because of the bright $[\text{OI}]\lambda 6300$ night sky line. The hydrogen lines $\text{H}\beta$, $\text{H}\gamma$, and $\text{H}\delta$ were also detected in the three brightest DIG spectra.

3.3. Search for HeI recombination line

The observations of strong $[\text{SII}](\lambda 6717 + \lambda 6730)$ and $[\text{NII}](\lambda 6548 + \lambda 6583)$ emission coupled with weak $[\text{OI}]\lambda 6300$ and $[\text{OIII}]\lambda 5007$ emission from the Reynolds layer within our Galaxy and the thick ionized layer surrounding NGC 891, imply that low ionization species dominate. While some ionization models are able to reproduce the observed line ratios, the hardness of the incident ionizing spectrum is a key to distinguishing between models. The $\text{HeI}\lambda 5876$ recombination line is sensitive to the spectral type of the ionizing star, since ionization of He requires stars of spectral type earlier than about O8 (Torres-Peimbert et al. 1974). This emission line is the strongest helium line in the visible regime, but is still extremely weak compared to $\text{H}\alpha$.

Fig. 3 shows the region around $\text{HeI}\lambda 5876$ in the spectrum of the “Bright” and “Moderate” DIG. The figure shows the red spectra prior to combination with the blue spectra. Because this region is close to the edge of the chip in the blue spectra, background subtraction was more difficult resulting in larger residuals for the night sky lines around HeI. The red spectrum of the “Bright” DIG shows a detection of $\text{HeI}\lambda 5876$. There is a feature in the blue spectrum consistent with the detection of HeI at the same strength as in the red spectrum, even though the night sky lines residuals are greater. The bright $\text{NaI}\lambda 5890 + \lambda 5896$ night sky lines just redward of HeI did not subtract perfectly, producing the obvious dip in baselevel. Although there are shifts of the emission features in the original spectra relative to the night sky lines amounting to about 5\AA because of M31’s galactic rotational velocity differences for various slit positions, the HeI line is always separated from this bright night sky line. However, a weaker OH molecular blend is blueward of HeI and sometimes blended with the line. This blend produces a broad pedestal in the “Moderate” DIG spectrum where we do not detect the HeI line, also shown in fig. 3. Because there is the possibility that this fainter night sky line could contribute to our estimate of the strength of the HeI line via a slight hump on the blue side of the HeI line, we consider our determination of the HeI line flux to be uncertain. To avoid a possible contribution from this hump we estimated the strength of the HeI line from the *peak* line intensity for HeI compared to $\text{H}\alpha$, as opposed to comparing total line fluxes. The measured ratio of $I_{\text{HeI}} / I_{\text{H}\alpha} = .045 \pm .015$. The upper limits from the other spectra are still consistent with this level of ionization, but, of course, also with lower levels of ionization of He. The sky subtraction produced sky line residuals in this region of the red

“Faint” and “Very Faint” spectra consistent with other regions, although not shown in fig. 3.

Our estimated ratio for $I_{\text{HeI}}/I_{\text{H}\alpha}$ is consistent with the value found for Galactic HII regions, .045 (Reynolds & Tufte 1995). This implies that stars of spectral type earlier than O7 are required to contribute to the ionization of the DIG. Reynolds & Tufte unsuccessfully searched for helium emission from two directions through the Reynolds layer. Their 2σ upper limit of $I_{\text{HeI}}/I_{\text{H}\alpha} = .012 \pm .006$ implies that He is primarily neutral and the radiation field is softer than previously thought. The two directions observed have surface brightness levels of about 30 pc cm^{-6} , the same as our “Moderate” spectra. Since, we are only able to place upper limits on $I_{\text{HeI}}/I_{\text{H}\alpha}$ for the “Moderate”, “Faint” and “Very Faint” DIG, the question remains open as to the hardness of the radiation field responsible for the fainter DIG. However, it appears that the radiation field present in the “Bright” DIG of M31 is harder than in Galactic DIG. This may result from the fact that our observations focus on DIG regions within the spiral arms of M31, while the Galactic observations sampled DIG farther from spiral arm structures.

Recent observations of ionized gas out of the plane of NGC 891 have found $I_{\text{HeI}}/I_{\text{H}\alpha} = .033$ (Rand 1996). This ratio suggests that helium is about 70% ionized and the equivalent stellar temperature of the radiation field is 37,500K, corresponding to spectral type O7. The consistency of these measurements with our estimation for the “Bright” DIG in M31 is somewhat surprising, especially given the discrepancy with Galactic DIG. Given that NGC 891 and the Milky Way are considered “twins”, with large ionized layers above the plane of each, one might expect the HeI line strength to be similar in the extraplanar DIG for these galaxies and possibly different for the DIG located within the plane of M31.

Also located in this spectral region is the [NII] λ 5755 line. This line is expected to be extremely weak, but important for temperature determination when compared to [NII] λ 6548 + λ 6583. Equation 5.5 of Osterbrock (1989), in the low-density limit (which is confirmed by [SII] lines), reads:

$$\frac{[\text{NII}]\lambda 6548 + [\text{NII}]\lambda 6583}{[\text{NII}]\lambda 5755} = 6.91 \exp\left(\frac{2.5 \times 10^4}{T}\right).$$

While we have no clear detection of the [NII] λ 5755 line even in the “Bright” DIG spectrum, we can estimate an upper limit to the temperature using the measured noise at the line position. The measured noise gave a 3σ upper limit on the line flux of $9.90 \times 10^{-16} \text{ erg s}^{-1} \text{ cm}^{-2}$. This noise limit does not place a strong constraint on the temperature of the DIG, but does suggest it is most likely below 17,000K.

4. Ionization Models & Discussion

By comparing the predictions of several ionization models and observations of DIG in the Galaxy to the observations of DIG in M31, we will attempt to address its ionization source. The pertinent line ratios from Galactic DIG and models discussed below are included in Table 1 for

comparison with the observed line ratios discussed above. Figures 4 and 5 are excitation diagrams which are useful in determining the model best able to fit the observed line ratios for DIG. Line ratios for several HII regions from our data set (Galarza et al. 1997) have been included to illustrate the striking differences from DIG regions. In particular, the $[SII](\lambda 6717 + \lambda 6731)/H\alpha$ ratio is at least a factor of 2 greater in the DIG compared to the compact HII regions, and the $[OII]\lambda 3727/H\alpha$ ratio on average is higher in the DIG than the compact HII regions.

4.1. Photoionization

At least for the solar neighborhood, Miller & Cox (1993) have shown that the observed O star distribution can supply the required ionizing radiation to produce the observed Galactic DIG. Mathis (1986) and Domgörgen & Mathis (1994) (hereafter DM) produced photoionization models based on the idea that diffuse stellar radiation is able to travel through a low-density ISM to ionize H far from high mass stars. The governing model parameters are X_{edge} , the fraction of neutral hydrogen at the model edge, and q , a measure of the mean ionizing photon density within the nebula to the mean electron density. Their “composite” models are a mixture of 20% $X_{edge}=.95$ gas (ie. edges of HI clouds), and 80% $X_{edge}=.1$ gas, which produces much of the $H\alpha$ emission. In this “composite” model, most of the emission is attributed to a low X_{edge} model because only these models produce the low $I_{[OI]}/I_{H\alpha}$ ratio observed in the Galactic DIG. Composite models were only published for $\log(q)$ in the range -3 to -4, which appears appropriate for the Galactic DIG. These composite models fit the observed $I_{[NII]}/I_{H\alpha}$ and $I_{[OII]}/I_{H\beta}$ ratio, although the observed values of $[OII]$ seem to have a larger scatter than model predictions (see fig 5). As is obvious from fig. 4, these composite models seem to slightly overpredict $[SII]$ while underpredicting $[OIII]$. The composite models were created to reproduce observations of the Galactic DIG, which has a low $I_{[OIII]}/I_{H\beta}$ ratio. Mathis (1996) has suggested that increasing $[OIII]$ in model predictions would be easy, since it was difficult to bring down the ratio to match Galactic DIG observations. Domgörgen & Mathis also published results for $X_{edge}=.10$ models alone, with a much larger range of q values. The $I_{[OII]}/I_{H\alpha}$ ratio was only published for $\log(q) = -3, -3.7, \text{ and } -4$ models, and showed a variation of less than 1% for these models. We therefore estimated the strength for other models to be the same. A model with $q=.005$ fits our observed line ratios the best, but values from .002 to .01 are consistent with the data. The larger q values imply a larger ratio of ionizing photons to gas density. Because the observed surface brightness of M31 DIG is in the same range as Galactic DIG ($5\text{-}35 \text{ pc cm}^{-6}$), we are not detecting systematically brighter DIG in M31. The difference in line ratios suggests that the conditions in M31 are somewhat different than in the Milky Way. The DIG regions we observed are primarily in spiral arms, while the Galactic DIG regions are not. The less diluted radiation field required to fit our observation may reflect the fact that there is a more prominent stellar radiation field within spiral arms. This is supported by the HeI detection in M31 compared to the upper limit found for Galactic DIG. We expect that the larger q value is the important factor in finding a model that fits our observations, not the specifics of “composite” or single X_{edge} model. Because we have no meaningful limits on $[OI]$, a low X_{edge} model is not

necessarily required. Results for a “composite” model for these larger q values would be valuable.

As can be seen in fig. 4, the DM models predict an increase in the $I_{[\text{SII}]} / I_{\text{H}\alpha}$ ratio with decreasing q parameter. If the q parameter appropriate for a given DIG region is related to the surface brightness of the region, then the models predict an increase in $I_{[\text{SII}]} / I_{\text{H}\alpha}$ with decreasing surface brightness. Just such a trend is observed in our representative spectra, and the individual spectra (Greenawalt et al. 1997). Ferguson et al. (1996a) have also seen a similar continuous range of $I_{[\text{SII}]} / I_{\text{H}\alpha}$ ratios from DIG to HII regions in the edge-on galaxy NGC 55. These observed trends would suggest that DIG and HII regions are intimately related by photoionization, and are actually two extremes in a continuous class of warm ionized gas structures. However, it is not clear why a similar trend of decreasing $I_{[\text{OIII}]} / I_{\text{H}\alpha}$ with increasing surface brightness is not seen as predicted by the DM models.

4.2. Mixing Layers

The turbulent mixing of hot and cool gas to produce warm gas at the boundary has been used by Slavin et al. (1993) (hereafter, SSB) to model some of the DIG in the Galaxy. They proposed that energy input from supernovae could be responsible for ionizing roughly 20% of the Galactic DIG. Hundreds of mixing layers along any given line of sight are thought to account for the observed surface brightness of ionized gas. The mixing speed of the hot gas and the temperature attained by the warm gas are important in the model. We compare to their Solar abundance models because the depleted abundance models predict elevated $[\text{SII}]$ line strengths which do not fit the observations as well. The predictions for models with $\log(\bar{T}) = 5.0, 5.3,$ and 5.5 are denoted with an “S” in figs 4 & 5. At each temperature, two mixing speeds are presented ($v = 25$ & 100 km s^{-1}). Attributing all emission to mixing layers is not plausible, because an extremely specific choice of parameters is required to match the observations. As can be seen in figs 4 & 5, for the $\log(\bar{T}) = 5.3$ & 5.5 models, the $[\text{OIII}]$ predictions are an order of magnitude above the observed values, while the $[\text{OII}]$ line is a factor of 5 above the observed values. Lowering the temperature decreases the oxygen line strengths, but a small change in temperature produces a very drastic decrease in the line strengths. Lowering the temperature to $\log(\bar{T}) = 5.0$ (a factor of 2 or 3), brings the $[\text{OII}]$ strength to a comparable level to the observations. However, the $[\text{OIII}]$ line strength drops by two orders of magnitude, so that it is now seriously underpredicted, as is the $[\text{SII}]$ line strength. Given the extreme sensitivity of model predictions to this temperature range, a very specific set of model parameters would be required to fit the observations. However, such a specific choice of parameters may be unlikely to be valid for many DIG regions spread over a large portion of a spiral galaxy, which is what comprises our representative DIG spectra. Therefore, regardless of the energetic arguments, this model in itself appears unlikely to account for all observed DIG.

Given the above arguments, turbulent mixing is likely only responsible for a small fraction of the DIG ionization, with photoionization being the dominant source. Therefore, a mixture of the SSB and DM models may be a more accurate way of modelling the observed line ratios. Given the

predicted line ratios for the DM and SSB models it is straightforward to determine the predicted line ratios for a model which attributes a certain fraction of the ionization of the DIG to turbulent mixing layers and the remaining amount to photoionization. Specifically, the predicted line ratio will be $R = \sum f_i R_i$, where R_i is the predicted line ratio for a component that contributes the fraction f_i to the total ionization. We calculated line ratios for models that combined either the SSB $\log(\bar{T}) = 5.0$, $v = 100 \text{ km s}^{-1}$ model (labeled S_2 in figs. 4 & 5) or the $\log(\bar{T}) = 5.3$, $v = 25 \text{ km s}^{-1}$ model (labeled S_3) with the DM $X_{edge} = .1$ model with $q = .005$ (tick mark 6 in figs. 4 & 5). Calculations were made for 5%, 10%, 20%, and 30% contribution from turbulent mixing. Turbulent mixing at $v = 25 \text{ km s}^{-1}$ that results in gas with $\log(\bar{T}) = 5.3$ is unlikely to contribute more than 5% to the “Very Faint” DIG in M31 because the predicted $I_{[OIII]}/I_{H\alpha}$ ratio would be well above our observations. The predictions for this model do not match any other observations, except possibly the “Moderate” DIG if the contribution from turbulent mixing is at the few percent level. Turbulent mixing at $v = 100 \text{ km s}^{-1}$, resulting in gas with $\log(\bar{T}) = 5.0$, can contribute up to 20% and still be consistent with our observation of the DIG in M31. As can be seen in fig. 4, although up to 20% of the ionization can arise from turbulent mixing, smaller contributions fit our observations better. Models that attributed the remaining fraction of ionization to DM’s “composite” model with $\log(q) = -3.7$ instead of the $X_{edge} = .1$ model predicted $I_{[SII]}/I_{H\alpha}$, $I_{[OIII]}/I_{H\alpha}$, and $I_{[OII]}/I_{H\alpha}$ ratios that did not fit any observations.

4.3. Discussion

Recent spectroscopy of NGC 891 (Rand 1996) has shown that $I_{[NII]}/I_{H\alpha}$ varies from a value of .4, in the plane, to about 1.4, 3.5 kpc out of the plane. This is quite different than similar observations for NGC 4631 (Golla et al. 1996) which find that the ratio is never greater than .6 and decreases to .2 in the midplane. Comparison of our observations to this extraplanar ionized gas suggests that the bulk of the emission from the DIG we see in M31 is at or near the midplane. In M31, the $I_{[NII]}/I_{H\alpha}$ ratio for all DIG brightness levels is .3-.35. As this is near the values obtained for the midplane gas in edge-on galaxies, it is reasonable to believe that the bulk of the DIG in M31 is likely relatively close to the plane. Similarly, the ratios measured for $I_{[OIII]}/I_{H\alpha}$ in M31 are near the low end of the range of values determined by recent narrow band [OII] imaging of NGC 55 (Ferguson et al. 1996a), roughly .7 in the midplane to as high as 2 at about 1kpc above the disk. This also supports the idea that the DIG observed in M31 has spectral properties consistent with DIG near the midplane of edge-on galaxies, although differences in abundance between M31 and NGC 55 may play a role as well.

Several emission lines have been observed for the Reynolds layer of the Milky Way (eg. Reynolds 1984, 1985a, 1985b, Reynolds & Tuftte 1995). They are included in Table 1. The emission measures of most of these observations are in the same range as the observations we present here for M31. Likewise, some of the observed line ratios occupy the same range of values. For instance, $I_{[SII]}/I_{H\alpha}$ is generally observed to be higher in the Milky Way, but it is sometimes seen

as low, or lower, as in M31. Noted exceptions are the ratios $I_{[\text{OIII}]} / I_{\text{H}\beta}$ and $I_{\text{HeI}} / I_{\text{H}\alpha}$, which appear lower in the Galactic DIG than in M31. Photoionization models account for these differences in line ratios by requiring the DIG in the Galaxy to be subjected to a more diluted radiation field in comparison to the the DIG in M31. Given that the DIG we observed in M31 is located in or near the spiral arms, it is reasonable to assume that the stellar radiation field may be harder in comparison to Galactic DIG regions due to a higher fraction of direct stellar versus diffuse radiation. In addition, higher q could imply either higher intensity or somewhat lower n_e ; lower n_e is not likely (see Waltherbos & Braun 1994). Since the emission measures are similar for both sets of DIG, Galactic and M31, it may be that different photoionization environments are important in different DIG regions within a galaxy. Testing this hypothesis would require the analysis of DIG regions between and within the spiral arms of a nearby spiral galaxy looking for differences in spectroscopic properties at the same DIG brightness level.

5. Conclusions

We have obtained sensitive spectra of representative DIG within M31 at four surface brightness levels, ranging from 9-59 pc cm^{-6} , and of DIG specifically selected “far” from HII regions. From these spectra, we have measured $\text{H}\alpha$, $\text{H}\beta$, $\text{H}\gamma$, $\text{H}\delta$, $[\text{NII}]\lambda 6583$, $[\text{SII}](\lambda 6717 + \lambda 6731)$, $[\text{OIII}]\lambda 5007$, and $[\text{OII}]\lambda 3727$ line intensities. Our data represent a more complete set of line observations for DIG within the disk of an external galaxy than has been available before.

Our results are:

- We tentatively detect $\text{HeI}\lambda 5876$ in the average DIG spectra with $\text{EM} = 58.4 \text{ pc cm}^{-6}$. The observed ratio is $I_{\text{HeI}} / I_{\text{H}\alpha} = .045 \pm .015$ implying that helium is nearly 100% singly ionized. This is in contrast to the upper limits detected for Galactic DIG, which suggest that helium is predominantly neutral. The M31 DIG regions are located primarily near prominent spiral arms, while the Galactic DIG regions are not. One would expect that within DIG regions immediately surrounding a spiral arm, the stellar radiation field should be harder compared to DIG regions away from spiral arms, in agreement with our results. For fainter DIG, our He line strength upper limits are consistent with the He being either ionized or neutral.
- The photoionization models of Domgörgen & Mathis (1994), appropriate for DIG within the Galaxy, underpredict the $[\text{OIII}]$ flux while overpredicting the $[\text{SII}]$ flux for DIG in M31. However, a higher q model, where q characterizes the relative importance of the stellar radiation field compared to the diffuse nebular field, is able to reproduce the observations. The need for the larger q value to fit our observations may not be surprising given that the M31 DIG regions are primarily located near spiral arms.
- The observed forbidden line ratios suggest that turbulent mixing (Slavin et al. 1993) appears to contribute only a small fraction of the ionization of the DIG. In particular, models that

attribute a fraction of the ionization to $\log(\bar{T})= 5.3$, $v=25 \text{ km s}^{-1}$ turbulent mixing and the remaining amount to photoionization, can reasonably well fit the observations of the “Very Faint” DIG if the contribution from turbulent mixing is at most about 5%. The predicted line ratios do not match line ratios for brighter DIG levels discussed here. Conversely, $\log(\bar{T})= 5.0$, $v=100 \text{ km s}^{-1}$ turbulent mixing can contribute at most 20% of the ionization of DIG, but lower fractions give better fits.

We thank J. Mathis for discussion regarding the subject of this paper. This work has been supported by a grant from NSF (AST 9123777) to R. A. M. W., and a grant to B. G. from the New Mexico Space Grant Consortium. We also acknowledge support from the Research Corporation through a Cottrell Scholarship grant to R. A. M. W.

REFERENCES

- Dettmar, R.-J. 1990, *A&A*, 232, L15
- Dettmar, R.-J. 1992, *Fund. Cos. Phys.*, 15, 143
- Dettmar, R.-J. & Schulz, H. 1992, *ApJ*, 254, L25
- Domgörgen, H. and Mathis, J.S. 1994, *ApJ*, 428, 647
- Dove, J.B. & Shull, J.M., 1994, *ApJ*, 430, 222
- Ferguson, A.M.N., Wyse, R.F.G., and Gallagher, J.S. 1996a, astro-ph/9609125
- Ferguson, A.M.N., Wyse, R.F.G., Gallagher, J.S., and Hunter, D.A. 1996b, *AJ*, 111, 2265
- Galarza, V., Walterbos, R.A.M., Greenawalt, B.E., and Braun, R. 1997, in preparation
- Golla, G., Dettmar, R.-J., and Domgörgen, H. 1996, *A&A*, 313, 439
- Greenawalt, B.E., & Walterbos, R.A.M. 1997a, in preparation
- Greenawalt, B.E., & Walterbos, R.A.M. 1997b, in preparation
- Greenawalt, B.E., Walterbos, R.A.M., and Braun, R. 1997, in preparation
- Hester, J.J., & Kulkarni, S.R. 1990, in *The Interstellar Medium in External Galaxies*, edited by D. Hollenbach and H. Thronsen (NASA CP-3084), p.288
- Hoopes, C.G., Walterbos, R.A.M., and Greenawalt, B.E. 1996, *AJ*, 112, 1429
- Hunter, D.A. 1994a, *AJ*, 107, 565
- Hunter, D.A. 1994b, *AJ*, 108, 1658
- Hunter, D.A. 1996, *ApJ*, 457, 671
- Hunter, D.A., & Gallagher, J.S. 1990, *ApJ*, 362, 480
- Hunter, D.A., & Gallagher, J.S. 1992, *ApJ*, 391, L9

- Hunter, D.A., & Gallagher, J.S. 1996, preprint
- Hunter, D.A., Hawley, W.N., & Gallagher, J.S. 1993, *AJ*, 106, 1797
- Keppel, J.W., Dettmar, R.-J., Gallagher, J.S., & Roberts, M.S. 1991, *ApJ*, 374, 507
- Kulkarni, S.R., & Heiles, C.E. 1988, in *Galactic and Extragalactic Radio Astronomy*, edited by G.L. Verschuur and K.I. Kellerman (Springer, New York), p. 95
- Mathis, J.S. 1986, *ApJ*, 301, 423
- Mathis, J.S. 1996, private communication
- Miller, W.W. & Cox, D.P. 1993, *ApJ*, 417, 579
- Osterbrock, D.E. 1989, *Astrophysics of Gaseous Nebulae and Active Galactic Nuclei* (Mill Valley: University Science Books)
- Rand, R.J. 1994, in *Proceedings of IAU Joint Discussion 1*, ed. van der Hulst, J.M.
- Rand, R.J. 1996, preprint
- Rand, R.J., Kulkarni, S.R., & Hester, J.J. 1990, *ApJ*, 352, L1
- Rand, R.J., Kulkarni, S.R., & Hester, J.J. 1992, *ApJ*, 396, 97
- Raymond, J.C. 1979, *ApJS*, 39, 1
- Reynolds, R.J. 1984, *ApJ*, 282, 191
- Reynolds, R.J. 1985a, *ApJ*, 294, 256
- Reynolds, R.J. 1985b, *ApJ*, 298, L27
- Reynolds, R.J. 1990, in *The Galactic and Extragalactic Background Radiation*, IAU Symposium No. 139, edited by S. Bowyer and C. Leinert (Kluwer, Dordrecht), p. 157
- Reynolds, R.J. 1991, *ApJ*, 372, L17
- Reynolds, R.J. & Tufte, S.L. 1995, *ApJ*, 439, L17
- Savage, B.D. & Mathis, J.S. 1979, *ARA&A*, 17, 73
- Sciama, D.W. 1990, *ApJ*, 364, 549
- Sciama, D.W. 1993, *ApJ*, 409, L25
- Sciama, D.W. 1995, *ApJ*, 448, 667
- Shull, J.M. & McKee, C. 1979, *ApJ*, 227, 131
- Slavin, J.D., Shull, J.M., and Begelman, M.C. 1993, *ApJ*, 407, 83
- Torres-Peimbert, S., Lazcano-Araujo, A., & Peimbert, M. 1974, *ApJ*, 191, 401
- Walterbos, R.A.M. & Braun, R. 1992, *A&AS*, 92, 625
- Walterbos, R.A.M. & Braun, R. 1994, *ApJ*, 431, 156
- Walterbos, R.A.M., King, N., & Braun, R. 1996, submitted to *ApJ*

Walterbos, R.A.M. & Schwering, P.B.W. 1987, A&AS, 66, 505

TABLE 1
SPECTROSCOPIC PROPERTIES OF DIG IN M31^a

	“Bright”	“Moderate”	“Faint”	“Very Faint”	“Far” ^b	Galactic ^c	DM Model ^d		ML Model ^g	
							“composite” ^e	“best fit” ^f	log(\bar{T})=5.0 ^h	log(\bar{T})=5.3 ⁱ
EM (pc cm ⁻⁶) ^{j,k}	58.4±8.2	33.7±6.2	17.7±3.3	9.1±3.5	22.6±6.7	2-80	–	–	–	–
H α /H β ^k	3.62±.06	3.50±.09	3.64±.16	4.38±.38	3.75±.15	–	–	–	3.31	2.69
[NII](λ 6583)/H α	.34±.01	.36±.01	.30±.02	.34±.06	.40±.02	.3-.5	.34-.35	.31	.19	.43
[SII](λ 6717 + 6731)/H α	.41±.01	.46±.02	.46±.03	.53±.06	.60±.03	.35-.85	.63-.78	.45	.21	.49
[SII](λ 6717)/[SII](λ 6731)	1.56±.09	1.54±.12	1.50±.18	1.35±.30	1.24±.11	–	–	–	1.47	1.45
[SII](λ 6717)/[NII](λ 6583)	.73±.03	.77±.04	.93±.10	.89±.18	.83±.06	.8	1.12-1.34	.87	.66	.67
[OIII](λ 5007)/H α	.15±.01	.20±.01	.12±.01	.21±.03	.17±.01	.06	.05-.10	.15	.01	1.67
[OII](λ 3727)/H α	.93±.03	.92±.04	1.17±.08	1.43±.20	1.20±.08	–	1.12	–	1.03	4.07

^aLine ratios corrected for reddening. Uncertainties in line ratios reflect errors in the mean; intrinsic scatter from one region to the next is significantly larger.

^bDIG regions “far” from bright HII regions, see text.

^cObserved values for Galactic DIG, (Reynolds 1984,1985a,1985b)

^dDomgörgen & Mathis 1994

^e20%($X_{edge}=.95$)+80%($X_{edge}=.10$), $q=.0001-.001$,Orion nebula abundances

^f $X_{edge}=.10$, $q=.005$, Orion nebula abundances

^gMixing Layer Model - Slavin et al. 1993

^hVelocity of hot gas relative to cold gas, $v=100$ km s⁻¹

ⁱVelocity of hot gas relative to cold gas, $v=25$ km s⁻¹

^j“Uncertainties refer to 1 σ rms spread in the distribution of intensities of individual spectra.

^kObserved values are uncorrected for reddening.

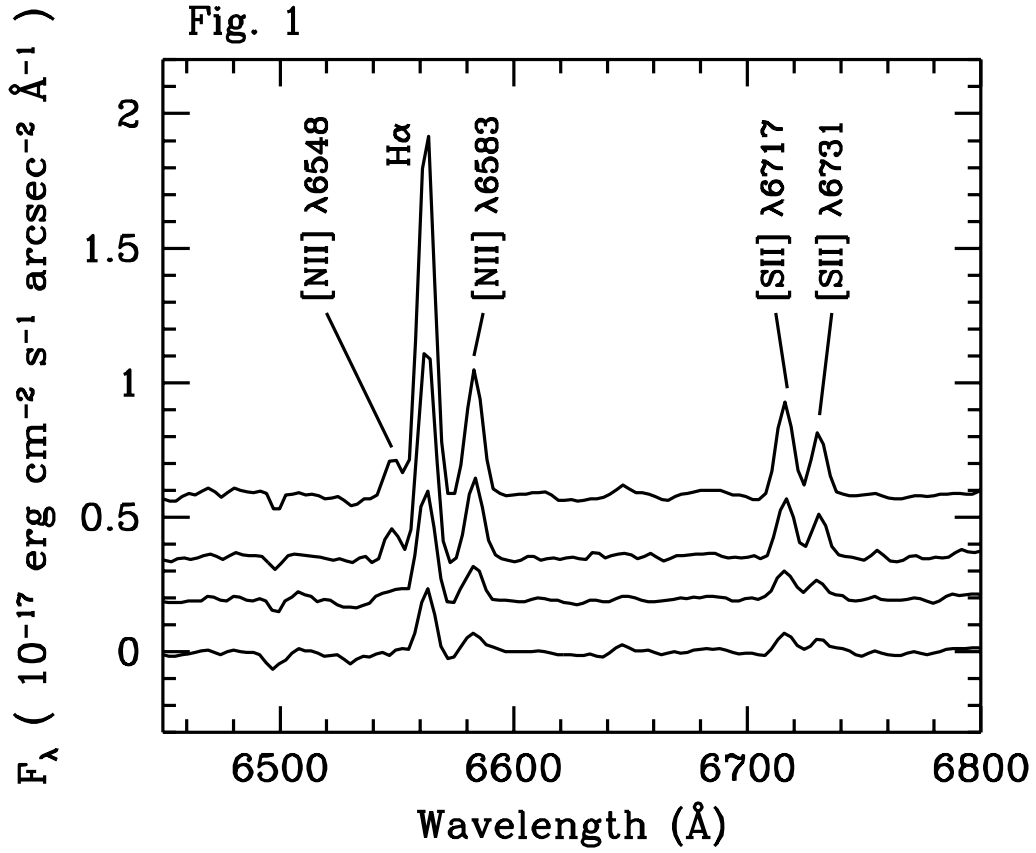


Fig. 1.— Co-added red spectra of representative DIG regions in M31. This spectral region includes lines of $\text{H}\alpha$, $[\text{NII}](\lambda 6548 + \lambda 6583)$, and $[\text{SII}](\lambda 6717 + \lambda 6731)$. The spectra shown, from top to bottom, are the “Bright”, “Moderate”, “Faint” and “Very Faint” DIG. A constant offset was added to the “Bright”, “Moderate”, and “Faint” spectra. Many night sky lines blueward of $\text{H}\alpha$ cause problems with the $[\text{NII}]\lambda 6548$ line determination and the dip in the baseline at $\sim 6500\text{\AA}$. The $[\text{SII}]$ emission is enhanced in DIG compared to HII regions, while $[\text{NII}]$ is at roughly the same level. All DIG spectra were shifted to account for the systemic and rotational velocity of M31 before co-adding.

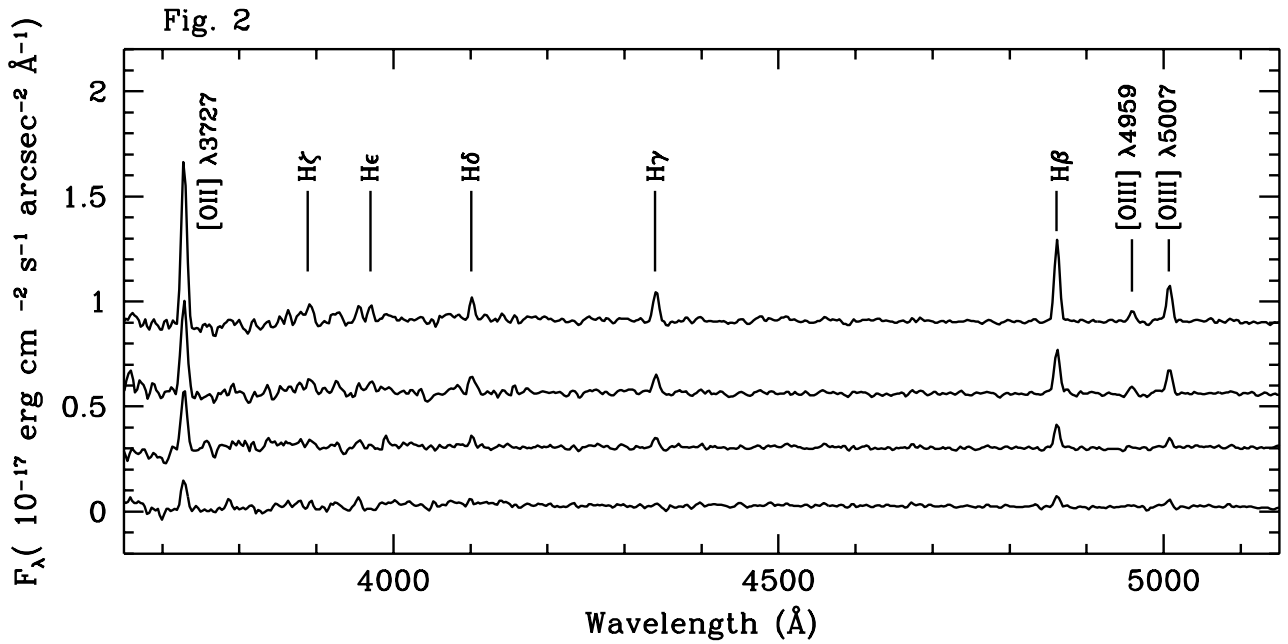


Fig. 2.— Co-added blue spectra of representative DIG regions in M31. Only the “blue” spectra contain observations blueward of 4000\AA , thus causing the decreased signal-to-noise (see text). The spectra shown, from top to bottom, are the “Bright”, “Moderate”, “Faint”, and “Very Faint” DIG. A constant offset was added to the “Bright”, “Moderate”, and “Faint” spectra. Besides the hydrogen lines in this region, we have clear detections of [OII] $\lambda 3727$, and [OIII] $\lambda 5007$ in all 4 DIG brightness levels. All DIG spectra have been shifted to account for the systemic and rotational velocity of M31 before co-adding.

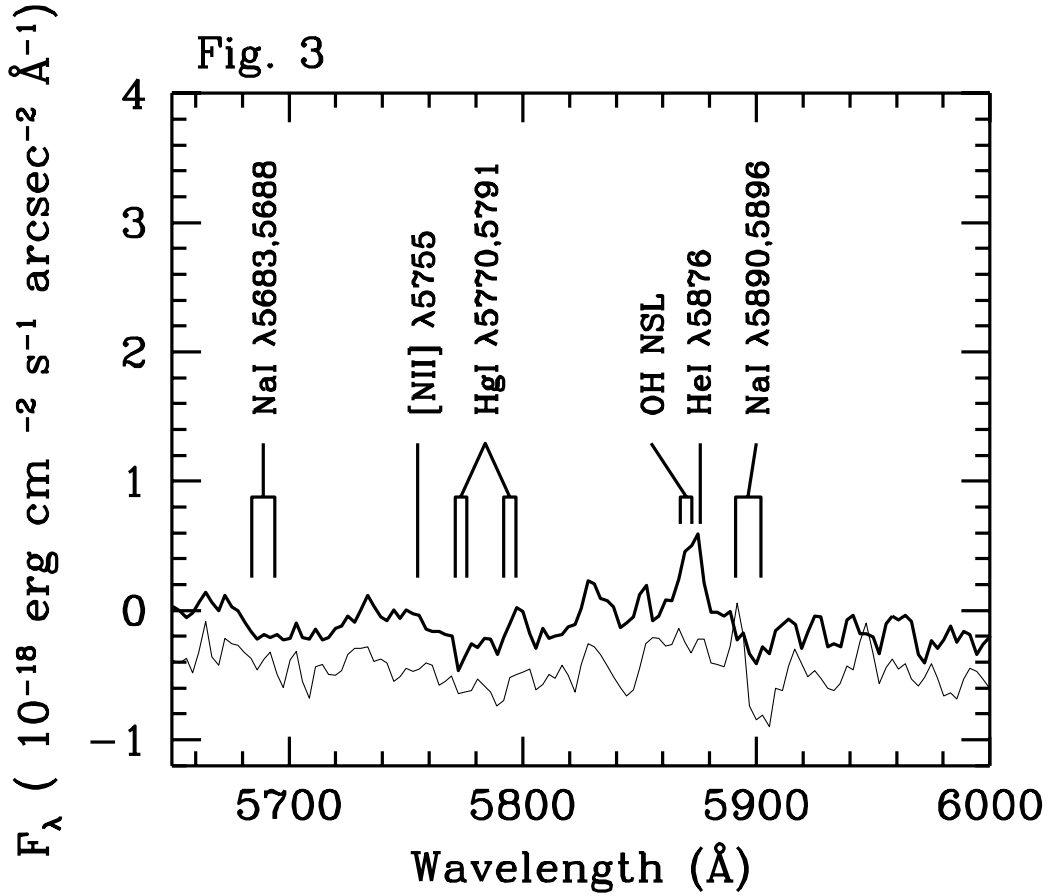


Fig. 3.— Observed “red” spectra of representative DIG in M31. The thick lined spectrum is the “Bright” DIG, while the thin lined spectrum is the “Moderate” DIG. The locations of the HeI and the [NII] λ 5755 lines are shown along with the location of several important night sky lines in this spectral region. There is some correlated “noise” between the two spectra because of night sky line residuals.

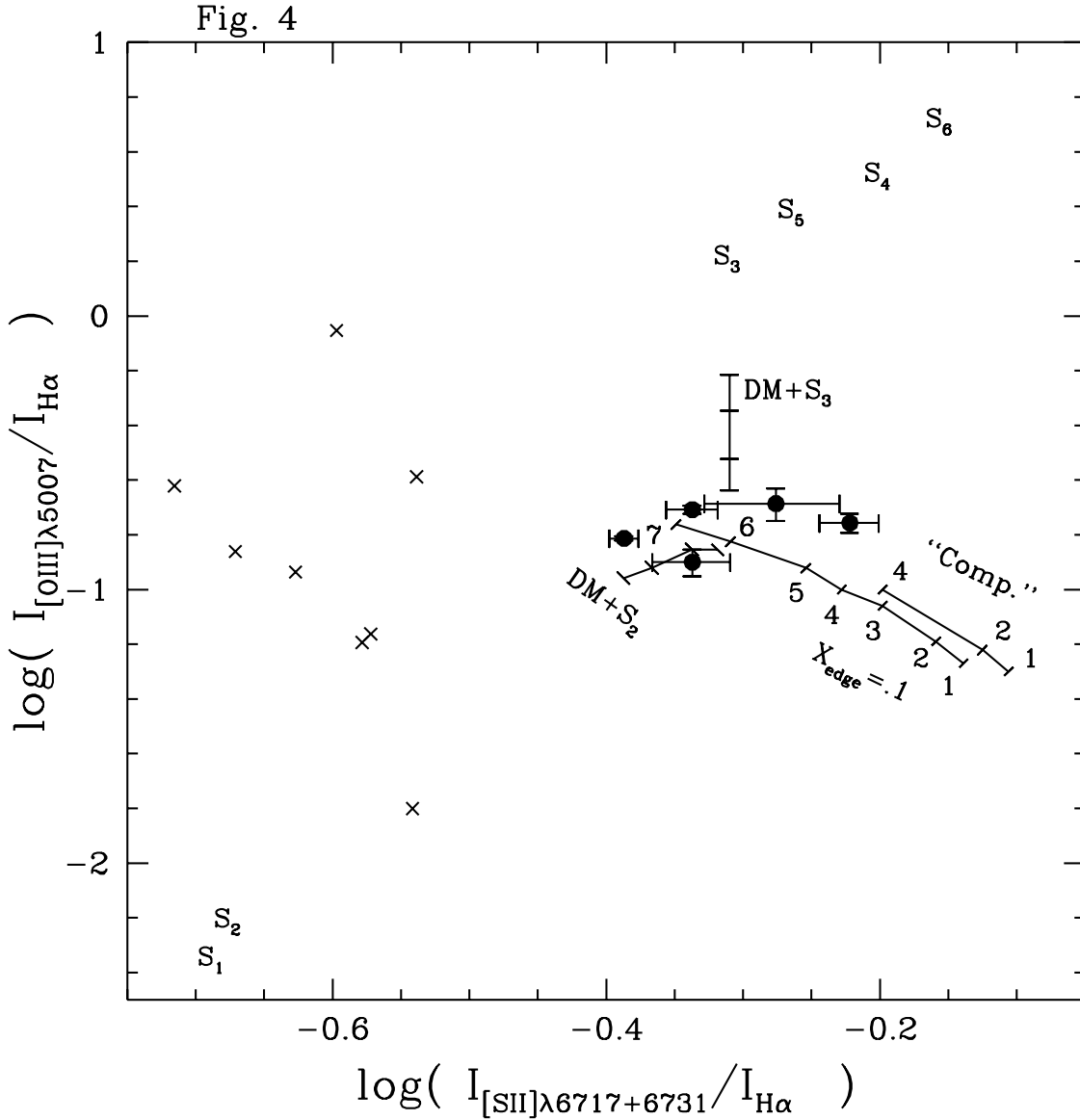


Fig. 4.— $I_{[SII]}/I_{H\alpha}$ vs. $I_{[OIII]}/I_{H\alpha}$ for representative DIG (filled circles) in M31. The \times 's are some HII regions from M31 (Galarza et al. 1997). The loci of line ratio predictions from the Domgörgen & Mathis (1994) models are label “Comp.” and $X_{edge}=.1$; the tick mark labels 1-7 refer to the $\log(q)$ values of -4,-3.7,-3.3,-3,-2.7,-2.3,-2, respectively. The mixing layer models with solar abundance (Slavin et al. 1993) are labeled with S's. The subscripts 1,2 correspond to $\log(\bar{T})=5.0$ models, while 3,4 and 5,6 correspond to $\log(\bar{T})=5.3$ & 5.5 models respectively. Odd subscripts are for models of mixing speed 25 km s^{-1} , while even subscripts are for 100 km s^{-1} models. Finally, the loci of predictions for the combined photoionization/mixing layer models discussed in the text are labeled DM+S₂ and DM+S₃. Tick marks correspond to 5%, 10%, 20%, and 30% contribution from mixing layers.

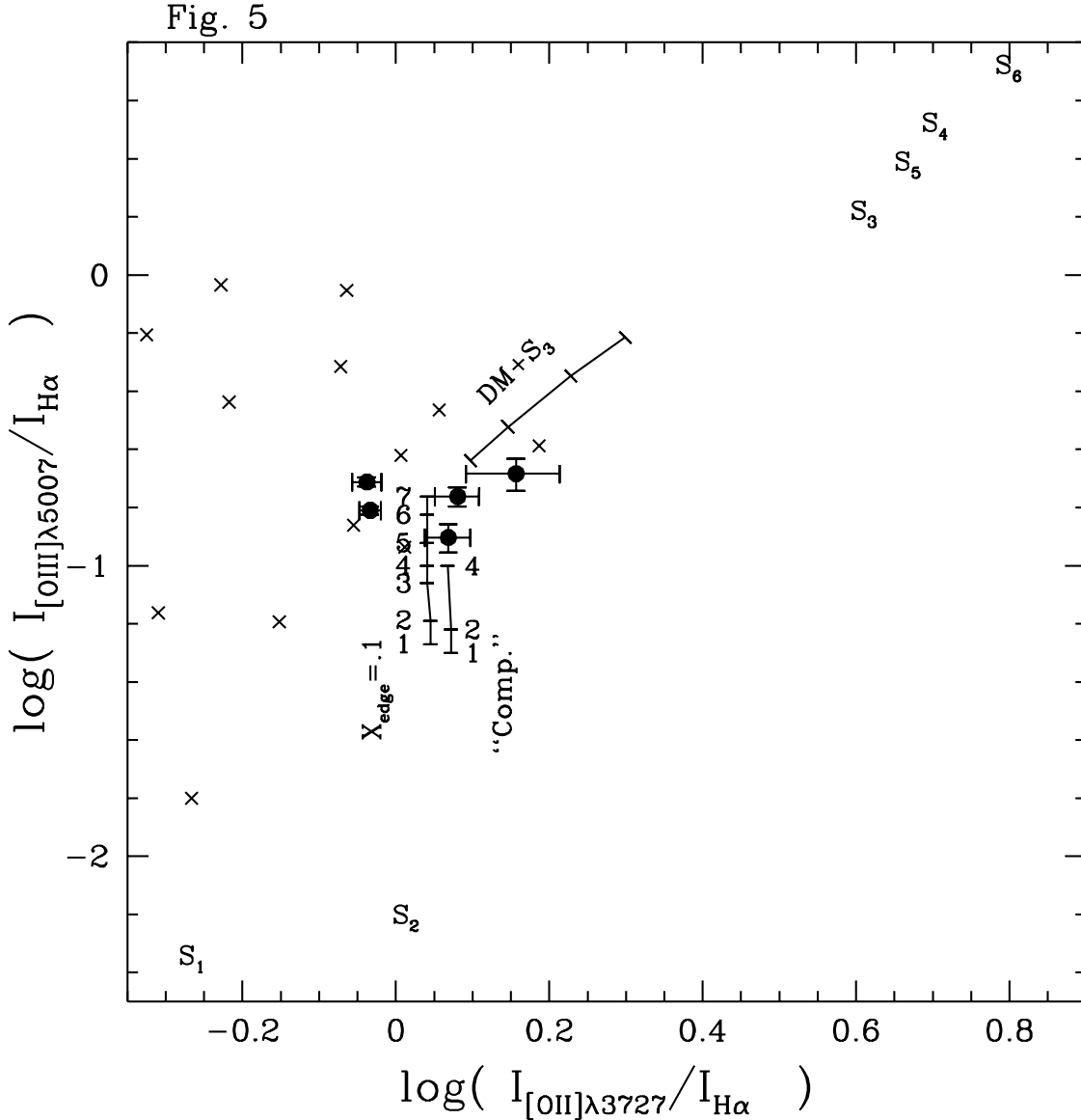


Fig. 5.— $I_{[OII]}/I_{H\alpha}$ vs. $I_{[OIII]}/I_{H\alpha}$ for representative DIG (filled circles) in M31. The \times 's are some HII regions in M31 (Galarza et al. 1997). The loci of line ratio predictions from the Domgörgen & Mathis (1994) models are label “Comp.” and $X_{edge}=.1$; the tick mark labels 1-7 refer to the $\log(q)$ values of -4,-3.7,-3.3,-3,-2.7,-2.3,-2, respectively. The mixing layer models with solar abundance (Slavin et al. 1993) are labeled with S's. The subscripts 1,2 correspond to $\log(\bar{T})= 5.0$ models, while 3,4 and 5,6 correspond to $\log(\bar{T})= 5.3$ & 5.5 models respectively. Odd subscripts are for models of mixing speed 25 km s^{-1} , while even subscripts are for 100 km s^{-1} models. Finally, the locus of predictions for the combined photoionization/mixing layer models discussed in the text is labeled DM+S₃. Tick marks correspond to 5%, 10%, and 20% contribution from mixing layers. The results for DM+S₂ are not shown because they overlap the DM $X_{edge}=.1$ model predictions and fall between tick marks 4-6.